Tracking an Unknown Number of Targets Using Multiple Sensors: A Belief Propagation Method

Florian Meyer*, Paolo Braca*, Peter Willett†, and Franz Hlawatsch‡

*Centre for Maritime Research and Experimentation, La Spezia 19126, Italy ({florian.meyer,paolo.braca}@cmre.nato.int)
†Department of ECE, University of Connecticut, Storrs, CT 06269, USA (willett@engr.uconn.edu)
‡Institute of Telecommunications, TU Wien, 1040 Vienna, Austria (fhlawats@nt.tuwien.ac.at)

***Abstract*—We propose a multisensor method for tracking an unknown number of targets. Low computational complexity and very good scalability in the number of targets, number of sensors, and number of measurements per sensor are achieved by running a belief propagation (BP) message passing scheme on a suitably devised factor graph. Using a redundant formulation of data association uncertainty and "augmented target states" including target indicators allows the proposed BP method to leverage statistical independencies for a drastic reduction of complexity. The proposed method is shown to outperform previously proposed multisensor methods for multitarget tracking, including methods with a less favorable scaling behavior.**

***Index Terms*—Multitarget tracking, data association, belief propagation, message passing, factor graph, sensor network.**

I. Introduction

A. Multitarget Tracking

Multitarget tracking aims at estimating the time-varying states—e.g., positions—of moving objects (targets) [1]. Typically, the number of targets is unknown and there is a data association (measurement origin) uncertainty [1], [2]. Traditional multitarget tracking methods [1], [3] and their extensions to multiple sensors [4]–[6] model the target states as a random vector. These methods usually assume that the number of targets is fixed and known. Extensions of traditional methods that infer also target presence/absence include the joint integrated probabilistic data association (JIPDA) filter [7], the joint integrated track splitting (JITS) filter [8], and the search-initialize-track filter [9]. A more recent class of multitarget tracking methods is based on random finite sets and finite set statistics (FISST). This class includes the probability hypothesis density (PHD) filter [2], [10], [11], the cardinalized PHD (CPHD) filter [2], [12], [13], and the multi-Bernoulli (MB) filter [2], [14].

If targets are low-observable, i.e., exhibit a low signal-to-noise ratio, it may not be possible to detect and track them reliably with a single sensor. Theoretical results [15] suggest that the probability of detecting targets can be strongly increased by increasing the number of sensors. However, the computational complexity of optimum multisensor-multitarget tracking filters scales exponentially in the number of sensors and the number of measurements per sensor [16]–[18]. Computationally feasible multisensor-multitarget tracking filters include the iterator-corrector (C)PHD (IC-(C)PHD) filter [19], which computes measurements from different sensors sequentially, the approximate product multisensor (C)PHD filter [20], and the partition-based multisensor (C)PHD (MS-(C)PHD) filter [17]. However, these filters either perform approximations of unknown fidelity and thus may not be able to fully realize the performance gains offered by multiple sensors, or they still scale poorly in relevant system parameters. An additional drawback of the IC-(C)PHD filter is that its performance strongly depends on the order in which the sensors are processed [17], [19], [20]. Certain recently introduced FISST-based techniques for tracking an unknown number of targets, such as the (generalized) labeled MB filter [21], [22], the track-oriented marginal Bernoulli/Poisson (TOMB/P) filter [23], and the measurement-oriented marginal Bernoulli/Poisson (MOMB/P) filter [23], were developed only for a single sensor.

B. A Belief Propagation Method for Scalable Multisensor-Multitarget Tracking

Here, we propose a multisensor method for multitarget tracking that combines excellent performance with very good scalability in all relevant system parameters. The method is suitable for an unknown, time-varying number of targets (although it requires the specification of a *maximally possible* number of targets) and implicitly performs track management. Our approach to multisensor-multitarget tracking is to perform ordered estimation using belief propagation (BP) message passing [24]–[26]. Whereas most FISST-based algorithms calculate an approximation of the *joint* posterior multiobject probability density function (pdf), BP provides accurate approximations of the *marginal* posterior pdfs for the individual targets. These approximations are then used to perform Bayesian detection and state estimation.

Our starting-point is the formulation of a Bayesian detection-estimation problem that involves the target states, target existence variables, and measurement-target association variables for all times, targets, and sensors. We use the formulation of data association uncertainty proposed in [27] and [28], and "augmented target states" in which the continuous states are complemented by binary variables indicating target existence. In contrast to FISST-based techniques, the joint

augmented target state is ordered and has a fixed number of components. This specific formulation allows the use of a BP algorithm [24]–[26], which leverages statistical independencies of variables for a drastic reduction of computational complexity. Particle-based calculations of all messages and beliefs make the proposed algorithm suited to arbitrary nonlinear and non-Gaussian measurement and state evolution models.

Message passing algorithms have been previously proposed for pure data association, i.e., without multitarget tracking or with multitarget tracking outside the message passing scheme [27]–[30]. To the best of our knowledge, the only existing BP methods for multisensor-multitarget tracking (including data association) are the one in [31] and our previous method in [32], which both assume a known number of targets. In [31], all target states and association variables at one time step are modeled as a joint state. Thus, the factor graph is tree-structured and BP message passing is exact but this comes at the cost of poor scalability in the number of targets. Apart from allowing for an unknown number of targets, our proposed method differs from [31] in that it employs the BP formulation of data association proposed in [27], [28]. Furthermore, our method retains the favorable scaling properties of our previous method [32], i.e., its complexity scales only quadratically in the number of targets, linearly in the number of sensors, and linearly in the number of measurements per sensor (assuming a fixed number of message passing iterations). Simulation results in a challenging scenario demonstrate that the performance of our method compares well with that of state-of-the-art methods, including methods with a less favorable scaling behavior (such as the CPHD filter, which scales cubically in the number of measurements and in the number of targets). In particular, our method can outperform the IC-(C)PHD filter [2], [19], an IC extension of the MB filter in [14], and the MS-(C)PHD filter [17].

C. Paper Organization

This paper is organized as follows. The system model and a statistical formulation are described in Section II. The proposed method is developed in Section III. Simulation results are reported in Section IV.

II. System Model and Statistical Formulation

A. Targets

We consider K *potential targets* $k \in \mathcal{K} \triangleq \{1, \ldots, K\}$. The existence of potential target k at time n is modeled by a Bernoulli variable $r_{n,k} \in \{0, 1\}$, i.e., target k exists at time n if and only if $r_{n,k} = 1$. The state $\mathbf{x}_{n,k}$ of potential target k at time n consists of the target's position and possibly further parameters. It will be convenient to formally consider a target state $\mathbf{x}_{n,k}$ also if $r_{n,k} = 0$, but of course the states of nonexisting targets are irrelevant. We define the *augmented state* as $\mathbf{y}_{n,k} \triangleq [\mathbf{x}_{n,k}^{\mathrm{T}}\ r_{n,k}]^{\mathrm{T}}$, and the *joint augmented state* as $\mathbf{y}_n \triangleq \left[\mathbf{y}_{n,1}^{\mathrm{T}} \cdots \mathbf{y}_{n,K}^{\mathrm{T}}\right]^{\mathrm{T}}$. We also define $\mathbf{r}_n \triangleq \left[r_{n,1} \cdots r_{n,K}\right]^{\mathrm{T}}$.

Let us, for the moment, denote a pdf or BP message defined for an augmented state generically as $\phi(\mathbf{y}_{n,k}) = \phi(\mathbf{x}_{n,k}, r_{n,k})$. Because the state $\mathbf{x}_{n,k}$ of a nonexisting target k (i.e., for $r_{n,k} = 0$) is irrelevant, we have

$$\phi(\mathbf{x}_{n,k}, 0) = \phi_{n,k}\, f_{\mathrm{D}}(\mathbf{x}_{n,k}), \tag{1}$$

where $f_{\mathrm{D}}(\mathbf{x}_{n,k})$ is a "dummy pdf." The form (1) must be preserved by a message multiplication operation (cf. [24, Eq. 5]), which implies the idempotency property $f_{\mathrm{D}}^2(\mathbf{x}_{n,k}) = f_{\mathrm{D}}(\mathbf{x}_{n,k})$. Because $f_{\mathrm{D}}(\mathbf{x}_{n,k})$ must integrate to one, it follows that $f_{\mathrm{D}}(\mathbf{x}_{n,k})$ is 1 on an arbitrary support $\mathcal{S}$ of area/volume $|\mathcal{S}| = 1$, and 0 outside $\mathcal{S}$. Defining

$$\phi(r_{n,k}) \triangleq \int \phi(\mathbf{x}_{n,k}, r_{n,k})\, \mathrm{d}\mathbf{x}_{n,k}, \tag{2}$$

we have for $r_{n,k} = 0$

$$\phi(0) = \int \phi(\mathbf{x}_{n,k}, 0)\, \mathrm{d}\mathbf{x}_{n,k} = \phi_{n,k} \int f_{\mathrm{D}}(\mathbf{x}_{n,k})\, \mathrm{d}\mathbf{x}_{n,k} = \phi_{n,k}. \tag{3}$$

Furthermore, it follows from (2) and (3) that

$$\sum_{r_{n,k} \in \{0,1\}} \int \phi(\mathbf{x}_{n,k}, r_{n,k})\, \mathrm{d}\mathbf{x}_{n,k} = \phi_{n,k} + \phi(1).$$

Thus, if $\phi(\mathbf{x}_{n,k}, r_{n,k})$ is a pdf in the sense that it is normalized, i.e., $\sum_{r_{n,k} \in \{0,1\}} \int \phi(\mathbf{x}_{n,k}, r_{n,k})\, \mathrm{d}\mathbf{x}_{n,k} = 1$, then $\phi_{n,k} + \phi(1) = 1$. In that case, $\phi_{n,k} = \phi(0)$ and $\phi(1)$ can be interpreted as, respectively, nonexistence and existence probabilities for potential target k, i.e., $\phi_{n,k} = \phi(0) = \Pr[r_{n,k} = 0]$ and $\phi(1) = \Pr[r_{n,k} = 1]$.

At time $n = 0$, the augmented target states $\mathbf{y}_{0,k}$ are assumed statistically independent (across k) with prior pdfs $f(\mathbf{y}_{0,k}) = f(\mathbf{x}_{0,k}, r_{0,k})$, and for $n \geq 0$, they are assumed to evolve independently according to Markovian dynamic models [1], [2]. Thus, the pdf of $\mathbf{y} \triangleq \left[\mathbf{y}_0^{\mathrm{T}} \cdots \mathbf{y}_n^{\mathrm{T}}\right]^{\mathrm{T}}$ factorizes as

$$f(\mathbf{y}) = \prod_{k=1}^{K} f(\mathbf{y}_{0,k}) \prod_{n'=1}^{n} f(\mathbf{y}_{n',k} | \mathbf{y}_{n'-1,k}), \tag{4}$$

where the single-target augmented state transition pdf $f(\mathbf{y}_{n,k} | \mathbf{y}_{n-1,k}) = f(\mathbf{x}_{n,k}, r_{n,k} | \mathbf{x}_{n-1,k}, r_{n-1,k})$ is given as follows. If $r_{n-1,k} = 0$, then $r_{n,k} = 1$ with probability $p_{n,k}^{\mathrm{b}}$ (birth probability), and for $r_{n,k} = 1$, $\mathbf{x}_{n,k}$ is distributed according to the birth pdf $f_{\mathrm{b}}(\mathbf{x}_{n,k})$. Thus,

$$f(\mathbf{x}_{n,k}, r_{n,k} | \mathbf{x}_{n-1,k}, 0) = \begin{cases} (1 - p_{n,k}^{\mathrm{b}})\, f_{\mathrm{D}}(\mathbf{x}_{n,k}), & r_{n,k} = 0 \\ p_{n,k}^{\mathrm{b}}\, f_{\mathrm{b}}(\mathbf{x}_{n,k}), & r_{n,k} = 1. \end{cases} \tag{5}$$

If $r_{n-1,k} = 1$, then $r_{n,k} = 1$ with probability $p_{n,k}^{\mathrm{s}}$ (survival probability), and for $r_{n,k} = 1$, $\mathbf{x}_{n,k}$ is distributed according to the state transition pdf $f(\mathbf{x}_{n,k} | \mathbf{x}_{n-1,k})$. Thus,

$$f(\mathbf{x}_{n,k}, r_{n,k} | \mathbf{x}_{n-1,k}, 1) = \begin{cases} (1 - p_{n,k}^{\mathrm{s}})\, f_{\mathrm{D}}(\mathbf{x}_{n,k}), & r_{n,k} = 0 \\ p_{n,k}^{\mathrm{s}}\, f(\mathbf{x}_{n,k} | \mathbf{x}_{n-1,k}), & r_{n,k} = 1. \end{cases} \tag{6}$$

A strategy for choosing $p^{\mathrm{b}}_{n,k}$, $p^{\mathrm{s}}_{n,k}$, and $f_{\mathrm{b}}(\mathbf{x}_{n,k})$ will be presented in an extended journal version of this paper [33]. Our previous work [32] is a special case of the present setup with $p^{\mathrm{s}}_{n,k}=1$ (existing targets always survive), $p^{\mathrm{b}}_{n,k}=0$ (no targets are born), and initial prior pdfs such that $\int f(\mathbf{x}_{0,k},1)\mathrm{d}\mathbf{x}_{0,k}=1$ (all targets exist at time $n=0$).

B. Sensors and Measurements

We consider S sensors $s\in\mathcal{S}\triangleq\{1,\ldots,S\}$. At time n, sensor s produces $M_n^{(s)}$ "thresholded" measurements $\mathbf{z}_{n,m}^{(s)}$, $m\in\mathcal{M}_n^{(s)}\triangleq\{1,\ldots,M_n^{(s)}\}$, which result from a detection process. We define $\mathbf{z}_n^{(s)}\triangleq\left[\mathbf{z}_{n,1}^{(s)\mathrm{T}}\cdots\mathbf{z}_{n,M_n^{(s)}}^{(s)\mathrm{T}}\right]^{\mathrm{T}}$, $\mathbf{z}_n\triangleq\left[\mathbf{z}_n^{(1)\mathrm{T}}\cdots\mathbf{z}_n^{(S)\mathrm{T}}\right]^{\mathrm{T}}$, and $\mathbf{m}_n\triangleq\left[M_n^{(1)}\cdots M_n^{(S)}\right]^{\mathrm{T}}$. There is a data association (measurement origin) uncertainty: it is not known which measurement $\mathbf{z}_{n,m}^{(s)}$ originated from which target k, and it is possible that $\mathbf{z}_{n,m}^{(s)}$ did not originate from any target (false alarm, clutter) or that a target did not lead to any measurement of sensor s (missed detection) [1], [2]. We assume that an existing target can generate at most one measurement at sensor s, and a measurement at sensor s can be generated by at most one existing target [1], [2]. The measurement-target associations at sensor s and time n can then be described by the random vector $\mathbf{a}_n^{(s)}=\left[a_{n,1}^{(s)}\cdots a_{n,K}^{(s)}\right]^{\mathrm{T}}$ with entries

$$a_{n,k}^{(s)}\triangleq\begin{cases}m\in\mathcal{M}_n^{(s)}, & \text{at time } n\text{, potential target } k \text{ generates measurement } m \text{ at sensor } s\\ 0, & \text{at time } n\text{, potential target } k \text{ is not detected by sensor } s.\end{cases}$$

We also define $\mathbf{a}_n\triangleq\left[\mathbf{a}_n^{(1)\mathrm{T}}\cdots\mathbf{a}_n^{(S)\mathrm{T}}\right]^{\mathrm{T}}$. An existing target k is detected by sensor s with probability $P_{\mathrm{d}}^{(s)}(\mathbf{x}_{n,k})$, which may depend on $\mathbf{x}_{n,k}$. Each false alarm measurement at sensor s is distributed according to the pdf $f_{\mathrm{FA}}\big(\mathbf{z}_{n,m}^{(s)}\big)$, and the number of false alarms is Poisson distributed with mean $\mu^{(s)}$.

Next, we derive the global likelihood function $f(\mathbf{z}|\mathbf{y},\mathbf{a},\mathbf{m})$, where $\mathbf{z}\triangleq\left[\mathbf{z}_1^{\mathrm{T}}\cdots\mathbf{z}_n^{\mathrm{T}}\right]^{\mathrm{T}}$, $\mathbf{a}\triangleq\left[\mathbf{a}_1^{\mathrm{T}}\cdots\mathbf{a}_n^{\mathrm{T}}\right]^{\mathrm{T}}$, and $\mathbf{m}\triangleq\left[\mathbf{m}_1^{\mathrm{T}}\cdots\mathbf{m}_n^{\mathrm{T}}\right]^{\mathrm{T}}$. Under the commonly used assumption [1], [2] that given $\mathbf{y}$, $\mathbf{a}$, and $\mathbf{m}$, the measurements $\mathbf{z}_n^{(s)}$ are conditionally independent across time n and sensor index s, the global likelihood function factorizes as

$$f(\mathbf{z}|\mathbf{y},\mathbf{a},\mathbf{m})=\prod_{n'=1}^{n}\prod_{s=1}^{S}f\big(\mathbf{z}_{n'}^{(s)}\big|\mathbf{y}_{n'},\mathbf{a}_{n'}^{(s)},M_{n'}^{(s)}\big). \tag{7}$$

Assuming furthermore that the different measurements $\mathbf{z}_{n,m}^{(s)}$, $m\in\mathcal{M}_n^{(s)}$ at any given sensor s are conditionally independent given $\mathbf{y}_n$, $\mathbf{a}_n^{(s)}$, and $M_n^{(s)}$, we have [1], [2]

$$f\big(\mathbf{z}_n^{(s)}\big|\mathbf{y}_n,\mathbf{a}_n^{(s)},M_n^{(s)}\big)=\left(\prod_{m=1}^{M_n^{(s)}}f_{\mathrm{FA}}\big(\mathbf{z}_{n,m}^{(s)}\big)\right)\times\prod_{k\in\mathcal{D}^{(s)}_{\mathbf{a}_n,\mathbf{r}_n}}\frac{f\Big(\mathbf{z}^{(s)}_{n,a_{n,k}^{(s)}}\Big|\mathbf{x}_{n,k}\Big)}{f_{\mathrm{FA}}\Big(\mathbf{z}^{(s)}_{n,a_{n,k}^{(s)}}\Big)}. \tag{8}$$

Here, $\mathcal{D}^{(s)}_{\mathbf{a}_n,\mathbf{r}_n}\triangleq\big\{k\in\mathcal{K}:r_{n,k}=1,a_{n,k}^{(s)}\neq0\big\}$ is the set of existing targets detected at sensor s and time n. Since $\mathbf{z}_n^{(s)}$ is observed and thus fixed, $M_n^{(s)}$ is also fixed and (8) can be written as

$$f\big(\mathbf{z}_n^{(s)}\big|\mathbf{y}_n,\mathbf{a}_n^{(s)},M_n^{(s)}\big)=C\big(\mathbf{z}_n^{(s)}\big)\prod_{k=1}^{K}g\big(\mathbf{x}_{n,k},r_{n,k},a_{n,k}^{(s)};\mathbf{z}_n^{(s)}\big), \tag{9}$$

where $C\big(\mathbf{z}_n^{(s)}\big)$ is a normalization factor that depends only on $\mathbf{z}_n^{(s)}$ and $g\big(\mathbf{x}_{n,k},r_{n,k},a_{n,k}^{(s)};\mathbf{z}_n^{(s)}\big)$ is defined as

$$g\big(\mathbf{x}_{n,k},1,a_{n,k}^{(s)};\mathbf{z}_n^{(s)}\big)=\begin{cases}\dfrac{f\big(\mathbf{z}_{n,m}^{(s)}\big|\mathbf{x}_{n,k}\big)}{f_{\mathrm{FA}}\big(\mathbf{z}_{n,m}^{(s)}\big)}, & a_{n,k}^{(s)}=m\in\mathcal{M}_n^{(s)}\\ 1, & a_{n,k}^{(s)}=0\end{cases}$$

$$g\big(\mathbf{x}_{n,k},0,a_{n,k}^{(s)};\mathbf{z}_n^{(s)}\big)=1. \tag{10}$$

The fact that the likelihood function in (9) factorizes with respect to the target states will be important for the development of the proposed BP algorithm in Section III.

Finally, by plugging (9) into (7), we obtain

$$f(\mathbf{z}|\mathbf{y},\mathbf{a},\mathbf{m})=C(\mathbf{z})\prod_{n'=1}^{n}\prod_{s=1}^{S}\prod_{k=1}^{K}g\big(\mathbf{x}_{n',k},r_{n',k},a_{n',k}^{(s)};\mathbf{z}_{n'}^{(s)}\big), \tag{11}$$

where $C(\mathbf{z})$ is a normalization factor that depends only on $\mathbf{z}$.

C. Joint Prior Distribution of Association Variables and Numbers of Measurements

Using the assumption that given $\mathbf{y}$, the $\mathbf{a}_n^{(s)}$ and the $M_n^{(s)}$ are conditionally independent across n and s [1], [2], the joint prior probability mass function (pmf) of $\mathbf{a}$ and $\mathbf{m}$ given $\mathbf{y}$ factorizes as

$$p(\mathbf{a},\mathbf{m}|\mathbf{y})=\prod_{n'=1}^{n}\prod_{s=1}^{S}p\big(\mathbf{a}_{n'}^{(s)},M_{n'}^{(s)}\big|\mathbf{y}_{n'}\big). \tag{12}$$

Furthermore, under the standard assumption that the measurements $\mathbf{z}_{n,m}^{(s)}$, $m\in\mathcal{M}_n^{(s)}$ of sensor s are shuffled by a random permutation, with each of the $M_n^{(s)}!$ possible permutations equally likely, it is shown in [1], [9] that $p\big(\mathbf{a}_n^{(s)},M_n^{(s)}\big|\mathbf{y}_n\big)$ factorizes as

$$\begin{aligned}&p\big(\mathbf{a}_n^{(s)},M_n^{(s)}\big|\mathbf{y}_n\big)\\ &=\psi\big(\mathbf{a}_n^{(s)}\big)\frac{e^{-\mu^{(s)}}(\mu^{(s)})^{M_n^{(s)}-|\mathcal{D}^{(s)}_{\mathbf{a}_n,\mathbf{r}_n}|}}{M_n^{(s)}!}\left(\prod_{k\in\mathcal{D}^{(s)}_{\mathbf{a}_n,\mathbf{r}_n}}P_{\mathrm{d}}^{(s)}(\mathbf{x}_{n,k})\right)\\ &\quad\times\prod_{k'\notin\mathcal{D}^{(s)}_{\mathbf{a}_n,\mathbf{r}_n}}\big[1\big(a_{n,k'}^{(s)}\big)-r_{n,k'}P_{\mathrm{d}}^{(s)}(\mathbf{x}_{n,k'})\big].\end{aligned} \tag{13}$$

Here, we introduced

$$\psi\big(\mathbf{a}_n^{(s)}\big)\triangleq\begin{cases}0, & \exists k,k'\in\mathcal{K}\text{ such that }a_{n,k}^{(s)}=a_{n,k'}^{(s)}\neq0\\ 1, & \text{otherwise,}\end{cases}$$

which enforces our exclusion assumptions (i.e., each existing target can generate at most one measurement at sensor s, and each measurement at sensor s can be generated by at most one target). Furthermore, $1(a) = 1$ if $a = 0$ and 0 otherwise. We can rewrite (13) as

$$p\big(\mathbf{a}_n^{(s)}, M_n^{(s)}\big|\mathbf{y}_n\big) = C\big(M_n^{(s)}\big)\,\psi\big(\mathbf{a}_n^{(s)}\big) \times \prod_{k=1}^{K} h\big(\mathbf{x}_{n,k}, r_{n,k}, a_{n,k}^{(s)}; M_n^{(s)}\big), \quad (14)$$

where $C\big(M_n^{(s)}\big)$ is a normalization factor that depends only on $M_n^{(s)}$ and $h\big(\mathbf{x}_{n,k}, r_{n,k}, a_{n,k}^{(s)}; M_n^{(s)}\big)$ is defined as

$$h\big(\mathbf{x}_{n,k}, 1, a_{n,k}^{(s)}; M_n^{(s)}\big) = \begin{cases} \dfrac{P_{\mathrm{d}}^{(s)}(\mathbf{x}_{n,k})}{\mu^{(s)}}, & a_{n,k}^{(s)} \in \mathcal{M}_n^{(s)} \\ 1 - P_{\mathrm{d}}^{(s)}(\mathbf{x}_{n,k}), & a_{n,k}^{(s)} = 0 \end{cases}$$

$$h\big(\mathbf{x}_{n,k}, 0, a_{n,k}^{(s)}; M_n^{(s)}\big) = 1\big(a_{n,k}^{(s)}\big). \quad (15)$$

Following [28], we will use alongside with the "target-oriented" association vector $\mathbf{a}_n^{(s)}$ the "measurement-oriented" association vector $\mathbf{b}_n^{(s)} = \big[b_{n,1}^{(s)} \cdots b_{n,M_n^{(s)}}^{(s)}\big]^{\mathrm{T}}$, whose entries are defined as

$$b_{n,m}^{(s)} \triangleq \begin{cases} k \in \mathcal{K}, & \text{at time } n, \text{ measurement } m \text{ at sensor } s \\ & \text{is generated by potential target } k \\ 0, & \text{at time } n, \text{ measurement } m \text{ at sensor } s \\ & \text{is not generated by a potential target.} \end{cases}$$

We also define $\mathbf{b}_n \triangleq \big[\mathbf{b}_n^{(1)\mathrm{T}} \cdots \mathbf{b}_n^{(S)\mathrm{T}}\big]^{\mathrm{T}}$ and $\mathbf{b} \triangleq \big[\mathbf{b}_1^{\mathrm{T}} \cdots \mathbf{b}_n^{\mathrm{T}}\big]^{\mathrm{T}}$. Note that $\mathbf{b}$ is redundant since it can be derived from $\mathbf{a}$ and vice versa. However, using $\mathbf{b}$, $p(\mathbf{a}, \mathbf{m}|\mathbf{y})$ in (12) can be formally rewritten as

$$p(\mathbf{a}, \mathbf{b}, \mathbf{m}|\mathbf{y}) = \prod_{n'=1}^{n} \prod_{s=1}^{S} p\big(\mathbf{a}_{n'}^{(s)}, \mathbf{b}_{n'}^{(s)}, M_{n'}^{(s)}\big|\mathbf{y}_{n'}\big), \quad (16)$$

with the single-sensor prior pmfs (cf. (14))

$$p\big(\mathbf{a}_n^{(s)}, \mathbf{b}_n^{(s)}, M_n^{(s)}\big|\mathbf{y}_n\big) = C\big(M_n^{(s)}\big) \prod_{k=1}^{K} h\big(\mathbf{x}_{n,k}, r_{n,k}, a_{n,k}^{(s)}; M_n^{(s)}\big) \prod_{m=1}^{M_n^{(s)}} \Psi\big(a_{n,k}^{(s)}, b_{n,m}^{(s)}\big),$$

where

$$\Psi\big(a_{n,k}^{(s)}, b_{n,m}^{(s)}\big) \triangleq \begin{cases} 0, & a_{n,k}^{(s)} = m,\ b_{n,m}^{(s)} \neq k \\ & \text{or } b_{n,m}^{(s)} = k,\ a_{n,k}^{(s)} \neq m \\ 1, & \text{otherwise.} \end{cases}$$

Thus, Equation (16) can be expressed as

$$p(\mathbf{a}, \mathbf{b}, \mathbf{m}|\mathbf{y}) = C(\mathbf{m}) \prod_{n'=1}^{n} \prod_{s=1}^{S} \prod_{k=1}^{K} h\big(\mathbf{x}_{n',k}, r_{n',k}, a_{n',k}^{(s)}; M_{n'}^{(s)}\big) \times \prod_{m=1}^{M_{n'}^{(s)}} \Psi\big(a_{n',k}^{(s)}, b_{n',m}^{(s)}\big), \quad (17)$$

where $C(\mathbf{m})$ is a normalization factor that depends only on $\mathbf{m}$. The "redundant" factorization in (17) will be an important basis for our development of the proposed BP algorithm in Section III.

D. Target Detection and State Estimation

Our task is to determine if potential target $k \in \mathcal{K}$ exists (i.e., to detect the binary target existence variables $r_{n,k}$) and to estimate the states $\mathbf{x}_{n,k}$ of detected targets from the past and present measurements of all the sensors, i.e., from the total measurement vector $\mathbf{z}$. In the Bayesian setting, this essentially amounts to calculating the marginal posterior existence probabilities $p(r_{n,k} = 1|\mathbf{z})$ and the marginal posterior state pdfs $f(\mathbf{x}_{n,k}|r_{n,k} = 1, \mathbf{z})$. Potential target k is detected if $p(r_{n,k} = 1|\mathbf{z})$ is larger than a suitably chosen threshold P_{th} [34, Ch. 2]. For the detected targets k, an estimate of $\mathbf{x}_{n,k}$ is then provided by the minimum mean-square error (MMSE) estimator [34, Ch. 4]

$$\hat{\mathbf{x}}_{n,k}^{\mathrm{MMSE}} \triangleq \int \mathbf{x}_{n,k}\, f(\mathbf{x}_{n,k}|r_{n,k}=1, \mathbf{z})\, \mathrm{d}\mathbf{x}_{n,k}\,. \quad (18)$$

The marginal statistics $p(r_{n,k} = 1|\mathbf{z})$ and $f(\mathbf{x}_{n,k}|r_{n,k} = 1, \mathbf{z})$ underlying target detection and state estimation can be obtained from the marginal posterior pdf of the augmented target state $f(\mathbf{y}_{n,k}|\mathbf{z}) = f(\mathbf{x}_{n,k}, r_{n,k}|\mathbf{z})$ according to

$$p(r_{n,k}=1|\mathbf{z}) = \int f(\mathbf{x}_{n,k}, r_{n,k}=1|\mathbf{z})\, \mathrm{d}\mathbf{x}_{n,k}$$

and

$$f(\mathbf{x}_{n,k}|r_{n,k}=1, \mathbf{z}) = \frac{f(\mathbf{x}_{n,k}, r_{n,k}=1|\mathbf{z})}{p(r_{n,k}=1|\mathbf{z})},$$

respectively. Here, $f(\mathbf{x}_{n,k}, r_{n,k}|\mathbf{z})$ can be computed efficiently as described next.

III. The Proposed Method

The proposed multisensor-multitarget tracking method performs BP message passing on a specific factor graph [24], [26], which describes the factorization of the joint posterior pdf involving all relevant parameters.

A. Factor Graph

The marginal posterior pdfs $f(\mathbf{y}_{n,k}|\mathbf{z}) = f(\mathbf{x}_{n,k}, r_{n,k}|\mathbf{z})$ needed for detection and estimation are marginals of the joint posterior pdf $f(\mathbf{y}, \mathbf{a}, \mathbf{b}|\mathbf{z})$. For the following derivation of $f(\mathbf{y}, \mathbf{a}, \mathbf{b}|\mathbf{z})$ and the corresponding factor graph, we assume that the measurements $\mathbf{z}$ are observed and thus fixed, and $M_n^{(s)}$ and $\mathbf{m}$ denote the numbers of the observed measurements and

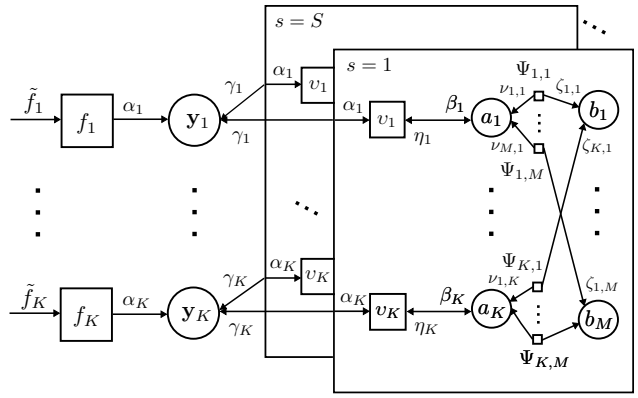

Fig. 1. Factor graph describing the factorization of $f(\mathbf{y}, \mathbf{a}, \mathbf{b}|\mathbf{z})$ in (19), shown for one time step. For simplicity, the time index n and sensor index s are omitted, and the following short notations are used: $f_k \triangleq f(\mathbf{y}_{n,k}|\mathbf{y}_{n-1,k})$, $\upsilon_k \triangleq \upsilon\big(\mathbf{y}_{n,k}, a_{n,k}^{(s)}; \mathbf{z}_n^{(s)}\big)$, $\tilde{f}_k \triangleq \tilde{f}(\mathbf{y}_{n,k})$, $\Psi_{k,m} \triangleq \Psi\big(a_{n,k}^{(s)}, b_{n,m}^{(s)}\big)$, $\alpha_k \triangleq \alpha(\mathbf{y}_{n,k})$, $\beta_k \triangleq \beta\big(a_{n,k}^{(s)}\big)$, $\eta_k \triangleq \eta\big(a_{n,k}^{(s)}\big)$, $\gamma_k \triangleq \gamma^{(s)}(\mathbf{y}_{n,k})$, $\nu_{m,k} \triangleq \nu_{m\to k}^{(p)}\big(a_{n,k}^{(s)}\big)$, and $\zeta_{k,m} \triangleq \zeta_{k\to m}^{(p)}\big(b_{n,m}^{(s)}\big)$.

the corresponding vector, respectively, i.e., they are fixed and consistent with $\mathbf{z}$. We then have

$$\begin{aligned} f(\mathbf{y}, \mathbf{a}, \mathbf{b}|\mathbf{z}) &= f(\mathbf{y}, \mathbf{a}, \mathbf{b}, \mathbf{m}|\mathbf{z}) \\ &\propto f(\mathbf{z}|\mathbf{y}, \mathbf{a}, \mathbf{b}, \mathbf{m})\, f(\mathbf{y}, \mathbf{a}, \mathbf{b}, \mathbf{m}) \\ &= f(\mathbf{z}|\mathbf{y}, \mathbf{a}, \mathbf{m})\, p(\mathbf{a}, \mathbf{b}, \mathbf{m}|\mathbf{y})\, f(\mathbf{y}). \end{aligned}$$

Here, we used Bayes' rule and the fact that $\mathbf{a}$ implies $\mathbf{b}$. Next, inserting (4) for $f(\mathbf{y})$, (11) for $f(\mathbf{z}|\mathbf{y}, \mathbf{a}, \mathbf{m})$, and (17) for $p(\mathbf{a}, \mathbf{b}, \mathbf{m}|\mathbf{y})$ yields

$$\begin{aligned} f(\mathbf{y}, \mathbf{a}, \mathbf{b}|\mathbf{z}) \propto \prod_{k=1}^{K} f(\mathbf{y}_{0,k}) \prod_{n'=1}^{n} f(\mathbf{y}_{n',k}|\mathbf{y}_{n'-1,k}) \\ \times \prod_{s=1}^{S} \upsilon\big(\mathbf{y}_{n',k}, a_{n',k}^{(s)}; \mathbf{z}_{n'}^{(s)}\big) \prod_{m=1}^{M_{n'}^{(s)}} \Psi\big(a_{n',k}^{(s)}, b_{n',m}^{(s)}\big), \end{aligned} \tag{19}$$

with

$$\begin{aligned} \upsilon\big(\mathbf{y}_{n,k}, a_{n,k}^{(s)}; \mathbf{z}_n^{(s)}\big) \triangleq g\big(\mathbf{x}_{n,k}, r_{n,k}, a_{n,k}^{(s)}; \mathbf{z}_n^{(s)}\big) \\ \times h\big(\mathbf{x}_{n,k}, r_{n,k}, a_{n,k}^{(s)}; M_n^{(s)}\big). \end{aligned} \tag{20}$$

The factor graph describing the factorization (19) is shown for one time step in Fig. 1.

B. BP Message Passing Algorithm

By running iterative BP message passing [24], [26] on the factor graph in Fig. 1, approximations ("beliefs") $\tilde{f}(\mathbf{y}_{n,k})$ of the marginal posterior pdfs $f(\mathbf{y}_{n,k}|\mathbf{z})$ can be obtained in an efficient way for all potential targets k. Since our factor graph contains loops, there is no general order in which the messages should be computed, and different orders may lead to different beliefs. The order underlying the proposed method is defined by the following rules: (i) Messages are only sent forward in time [35]. (ii) Iterative message passing is only performed for data association, and only at each time step and at each sensor separately, i.e., in particular, for the loops connecting different sensors we only perform a single message passing iteration.

These rules, combined with the generic BP rules for calculating messages and beliefs [24]–[26], lead to the following BP message passing operations at time n. First, a prediction step is performed for all potential targets $k \in \mathcal{K}$:

$$\begin{aligned} \alpha(\mathbf{x}_{n,k}, r_{n,k}) = \sum_{r_{n-1,k}\in\{0,1\}} \int f(\mathbf{x}_{n,k}, r_{n,k}|\mathbf{x}_{n-1,k}, r_{n-1,k}) \\ \times \tilde{f}(\mathbf{x}_{n-1,k}, r_{n-1,k})\, \mathrm{d}\mathbf{x}_{n-1,k}, \end{aligned} \tag{21}$$

where $\tilde{f}(\mathbf{x}_{n-1,k}, r_{n-1,k})$ was calculated at the previous time $n-1$. Inserting (5) and (6), the prediction step can be rewritten as follows: for $r_{n,k} = 1$,

$$\begin{aligned} \alpha(\mathbf{x}_{n,k}, 1) = p_{n,k}^{\mathrm{b}} f_{\mathrm{b}}(\mathbf{x}_{n,k})\, \tilde{f}_{n-1,k} \\ + p_{n,k}^{\mathrm{s}} \int f(\mathbf{x}_{n,k}|\mathbf{x}_{n-1,k}) \tilde{f}(\mathbf{x}_{n-1,k}, 1)\, \mathrm{d}\mathbf{x}_{n-1,k}, \end{aligned}$$

and for $r_{n,k} = 0$,

$$\alpha_{n,k} = \big(1 - p_{n,k}^{\mathrm{b}}\big)\tilde{f}_{n-1,k} + \big(1 - p_{n,k}^{\mathrm{s}}\big) \int \tilde{f}(\mathbf{x}_{n-1,k}, 1)\, \mathrm{d}\mathbf{x}_{n-1,k}.$$

Here, we recall from (3) that $\tilde{f}_{n-1,k} = \int \tilde{f}(\mathbf{x}_{n-1,k}, 0)\, \mathrm{d}\mathbf{x}_{n-1,k}$ and $\alpha_{n,k} = \int \alpha(\mathbf{x}_{n,k}, 0)\, \mathrm{d}\mathbf{x}_{n,k}$. From (21) and the fact that $\tilde{f}(\mathbf{x}_{n,k}, r_{n,k})$ is normalized, it follows that also $\alpha(\mathbf{x}_{n,k}, r_{n,k})$ is normalized, and thus $\alpha_{n,k} = 1 - \int \alpha(\mathbf{x}_{n,k}, 1)\, \mathrm{d}\mathbf{x}_{n,k}$.

Next, the following steps are performed for all potential targets $k \in \mathcal{K}$ and all sensors $s \in \mathcal{S}$ in parallel:

1) Measurement evaluation:

$$\begin{aligned} \beta\big(a_{n,k}^{(s)}\big) &= \sum_{r_{n,k}\in\{0,1\}} \int \upsilon\big(\mathbf{x}_{n,k}, r_{n,k}, a_{n,k}^{(s)}; \mathbf{z}_n^{(s)}\big) \\ &\qquad \times \alpha(\mathbf{x}_{n,k}, r_{n,k})\, \mathrm{d}\mathbf{x}_{n,k} \\ &= \int \upsilon\big(\mathbf{x}_{n,k}, 1, a_{n,k}^{(s)}; \mathbf{z}_n^{(s)}\big)\, \alpha(\mathbf{x}_{n,k}, 1)\, \mathrm{d}\mathbf{x}_{n,k} \\ &\qquad + 1\big(a_{n,k}^{(s)}\big)\, \alpha_{n,k}. \end{aligned}$$

Here, we used the fact that $\upsilon\big(\mathbf{x}_{n,k}, 0, a_{n,k}^{(s)}; \mathbf{z}_n^{(s)}\big) = 1\big(a_{n,k}^{(s)}\big)$ (cf. (20) and (10), (15)).

2) Iterative data association (following [27], [28], [36]): In iteration $p \in \{1, \ldots, P\}$, for all measurements $m \in \mathcal{M}_n^{(s)}$,

$$\nu_{m\to k}^{(p)}\big(a_{n,k}^{(s)}\big) = \sum_{b_{n,m}^{(s)}} \Psi\big(a_{n,k}^{(s)}, b_{n,m}^{(s)}\big) \prod_{k'\in\mathcal{K}\setminus\{k\}} \zeta_{k'\to m}^{(p-1)}\big(b_{n,m}^{(s)}\big) \tag{22}$$

and

$$\begin{aligned} \zeta_{k\to m}^{(p)}\big(b_{n,m}^{(s)}\big) = \sum_{a_{n,k}^{(s)}} \beta\big(a_{n,k}^{(s)}\big)\, \Psi\big(a_{n,k}^{(s)}, b_{n,m}^{(s)}\big) \\ \times \prod_{m'\in\mathcal{M}_n^{(s)}\setminus\{m\}} \nu_{m'\to k}^{(p)}\big(a_{n,k}^{(s)}\big). \end{aligned} \tag{23}$$

Here, e.g., $\sum_{b_{n,m}^{(s)}}$ is short for $\sum_{b_{n,m}^{(s)} \in \{0,\ldots,K\}}$. The iteration loop is initialized ($p=0$) by

$$\zeta_{k\to m}^{(0)}\big(b_{n,m}^{(s)}\big) = \sum_{a_{n,k}^{(s)}} \beta\big(a_{n,k}^{(s)}\big)\, \Psi\big(a_{n,k}^{(s)}, b_{n,m}^{(s)}\big). \tag{24}$$

An efficient implementation of (22) and (23) is described in [28] and [36]. After the last iteration $p=P$, all the $\nu_{m\to k}^{(P)}\big(a_{n,k}^{(s)}\big)$, $m \in \mathcal{M}_n^{(s)}$ are multiplied, i.e.,

$$\eta\big(a_{n,k}^{(s)}\big) = \prod_{m=1}^{M_n^{(s)}} \nu_{m\to k}^{(P)}\big(a_{n,k}^{(s)}\big). \tag{25}$$

3) Measurement update:

$$\gamma^{(s)}(\mathbf{x}_{n,k}, 1) = \sum_{a_{n,k}^{(s)}} \upsilon\big(\mathbf{x}_{n,k}, 1, a_{n,k}^{(s)}; \mathbf{z}_n^{(s)}\big)\, \eta\big(a_{n,k}^{(s)}\big)$$

$$\gamma_{n,k}^{(s)} = \eta\big(a_{n,k}^{(s)} = 0\big).$$

Finally, the beliefs $\tilde{f}(\mathbf{y}_{n,k}) = \tilde{f}(\mathbf{x}_{n,k}, r_{n,k})$ approximating the marginal posterior pdfs $f(\mathbf{y}_{n,k}|\mathbf{z}) = f(\mathbf{x}_{n,k}, r_{n,k}|\mathbf{z})$ are obtained as

$$\tilde{f}(\mathbf{x}_{n,k}, 1) = \frac{1}{C_{n,k}}\, \alpha(\mathbf{x}_{n,k}, 1) \prod_{s=1}^{S} \gamma^{(s)}(\mathbf{x}_{n,k}, 1) \tag{26}$$

$$\tilde{f}_{n,k} = \frac{1}{C_{n,k}}\, \alpha_{n,k} \prod_{s=1}^{S} \gamma_{n,k}^{(s)}, \tag{27}$$

with

$$C_{n,k} = \int \alpha(\mathbf{x}_{n,k}, 1) \prod_{s=1}^{S} \gamma^{(s)}(\mathbf{x}_{n,k}, 1)\, \mathrm{d}\mathbf{x}_{n,k} + \alpha_{n,k} \prod_{s=1}^{S} \gamma_{n,k}^{(s)}.$$

Note that we used $f_{\mathrm{D}}^2(\mathbf{x}_{n,k}) = f_{\mathrm{D}}(\mathbf{x}_{n,k})$ (cf. Section II-A) to obtain (27). The belief $\tilde{f}(\mathbf{x}_{n,k}, 1)$ in (26) provides an approximation of $f(\mathbf{x}_{n,k}, r_{n,k}=1|\mathbf{z})$ and can thus be used for Bayesian detection and estimation as discussed in Section II-D. A particle-based implementation of the above BP message passing algorithm that avoids the explicit evaluation of integrals and message products will be presented in the journal version of this paper [33].

The high accuracy of the "data association" iteration loop (22)–(25) has been demonstrated numerically [27], [28] (see also Section IV-B), and its convergence has been proven [28], [36]. As further analyzed in [33], the complexity of our method scales only quadratically in the number of targets, linearly in the number of sensors, and linearly in the number of measurements per sensor (assuming a fixed number P of message passing iterations).

IV. Simulation Results

We compare the performance of our method with that of five previously proposed methods for multisensor-multitarget tracking, and we study how certain parameters affect the performance.

A. Simulation Setup

We consider $K=8$ potential targets and up to five actual targets. The target states consist of two-dimensional (2D) position and velocity, i.e., $\mathbf{x}_{n,k} = [x_{1,n,k}\ x_{2,n,k}\ \dot{x}_{1,n,k}\ \dot{x}_{2,n,k}]^{\mathrm{T}}$. The region of interest (ROI) is $[-3000, 3000]\times[-3000, 3000]$. All existing targets move according to the constant-velocity motion model, i.e., $\mathbf{x}_{n,k} = \mathbf{A}\mathbf{x}_{n-1,k} + \mathbf{W}\mathbf{u}_{n,k}$, where the matrices $\mathbf{A} \in \mathbb{R}^{4\times4}$ and $\mathbf{W} \in \mathbb{R}^{4\times2}$ are chosen as in [37] and $\mathbf{u}_{n,k} \sim \mathcal{N}(\mathbf{0}, \sigma_u^2 \mathbf{I}_2)$ with $\sigma_u^2 = 0.025$ is an independent and identically distributed (iid) sequence of 2D Gaussian random vectors. The birth and survival probabilities are $p_{n,k}^{\mathrm{b}} = 0.01$ and $p_{n,k}^{\mathrm{s}} = 0.999$, respectively. We simulated a challenging scenario where the targets intersect at the ROI center. To obtain this behavior, we first assumed that the five targets start from initial positions uniformly placed on a circle of radius 1000 and move with an initial speed of 10 toward the ROI center. The actual trajectories were then obtained by letting the targets start to exist at times $n=5$, 10, 15, 20, and 25.

The sensor positions $\mathbf{p}^{(s)}$ are uniformly placed on a circle of radius 3000. The sensors perform range and bearing measurements within a range of 6000. More specifically, the target-generated measurements (within the measurement range) are given by

$$\mathbf{z}_{n,m}^{(s)} = \big[\, \big\|\tilde{\mathbf{x}}_{n,k} - \mathbf{p}^{(s)}\big\|\ \ \varphi\big(\tilde{\mathbf{x}}_{n,k}, \mathbf{p}^{(s)}\big)\,\big]^{\mathrm{T}} + \mathbf{v}_{n,m}^{(s)},$$

where $\tilde{\mathbf{x}}_{n,k} \triangleq [x_{1,n,k}\ \ x_{2,n,k}]^{\mathrm{T}}$, $\varphi\big(\tilde{\mathbf{x}}_{n,k}, \mathbf{p}^{(s)}\big)$ is the angle (in degrees) of the vector $\tilde{\mathbf{x}}_{n,k}$ relative to the vector $\mathbf{p}^{(s)}$, and $\mathbf{v}_{n,m}^{(s)} \sim \mathcal{N}(\mathbf{0}, \mathbf{C}_v)$ with $\mathbf{C}_v = \mathrm{diag}\{10^2, 0.5^2\}$ is an iid sequence of 2D Gaussian measurement noise vectors. The mean number of false alarm measurements is $\mu^{(s)} = 2$. The false alarm pdf $f_{\mathrm{FA}}\big(\mathbf{z}_{n,m}^{(s)}\big)$ is linearly increasing on $[0, 6000]$ and zero outside $[0, 6000]$ with respect to the range component and uniform on $[0, 360)$ with respect to the angle component. In Cartesian coordinates, the false alarm pdf is uniform on the sensor's measurement area.

We simulated a particle implementation of the proposed method—to be presented in the journal version of this paper [33]—in which each belief $\tilde{f}(\mathbf{x}_{n,k}, r_{n,k})$ is approximated by a set of particles and weights $\big\{\big(\mathbf{x}_{n,k}^{(j)}, w_{n,k}^{(j)}\big)\big\}_{j=1}^{J}$. We used $J=3000$ particles for each potential target. The sum of the weights, $p_{n,k}^{\mathrm{e}} \triangleq \sum_{j=1}^{J} w_{n,k}^{(j)}$, provides an approximation of the target existence probability $p(r_{n,k}=1|\mathbf{z})$, and potential target k is considered to exist (is detected) if $p_{n,k}^{\mathrm{e}} > 0.5$. For each detected target k, an approximation of the MMSE state estimate $\hat{\mathbf{x}}_{n,k}^{\mathrm{MMSE}}$ in (18) is then calculated as

$$\hat{\mathbf{x}}_{n,k} = \frac{1}{p_{n,k}^{\mathrm{e}}} \sum_{j=1}^{J} w_{n,k}^{(j)}\, \mathbf{x}_{n,k}^{(j)}.$$

We used $P=20$ BP iterations, simulated 150 time steps, and performed 400 simulation runs.

B. Performance Comparison

We compare the proposed method with particle implementations of the IC-PHD filter [2], [11], [19], the IC-CPHD filter

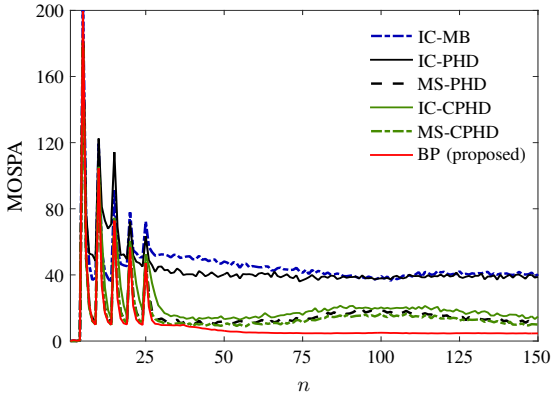

Fig. 2. MOSPA error versus time n for $S=3$ sensors and $P_{\mathrm{d}}=0.8$.

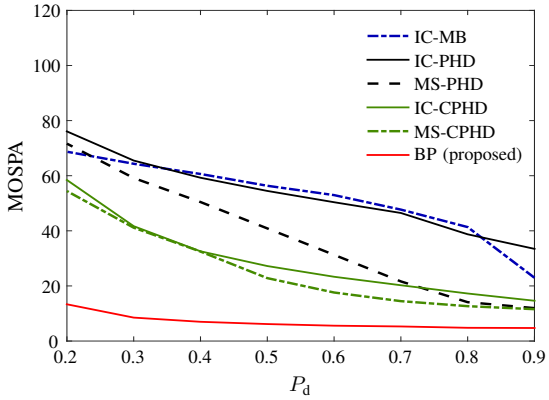

Fig. 3. Time-averaged MOSPA error versus P_{d} for $S=3$ sensors.

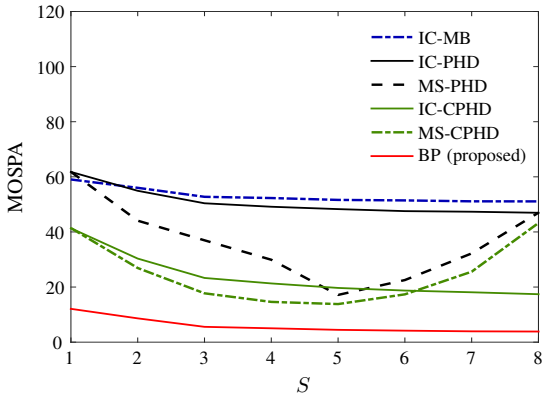

Fig. 4. Time-averaged MOSPA error versus number of sensors S for $P_{\mathrm{d}}=0.6$.

[2], [13], [19], the IC-MB filter [2], [14], and the partition-based MS-PHD and MS-CPHD filters [17]. Here, the "IC-" filters are simple multisensor extensions in which a single-sensor update step is performed sequentially for each sensor [2], [6], [19]. The partition-based MS-(C)PHD filters [17] are approximations of the exact multisensor (C)PHD filters that can achieve a better performance than the "IC-" filters at the cost of a higher computational complexity. We note that the exact multisensor (C)PHD filters are infeasible for the simulated scenario since their computational complexity scales exponentially in the number of sensors and in the number of measurements per sensor [16], [18], [38].

The (C)PHD-type filters perform kmeans++ clustering [39] for state estimation and use 24000 particles to represent the state pdf of the targets. The IC-MB filter uses 3000 particles for each Bernoulli component. In the MS-(C)PHD filter, similarly to [17], the maximum numbers of subsets and partitions are 120 and 720, respectively. With the above-mentioned parameters, the runtime of the proposed method is similar to that of the IC-PHD filter and shorter than that of the other simulated filters. At each time n, the birth intensities or pdfs of all methods are generated by using the previous measurement $\mathbf{z}_{n-1,m}^{(s')}$ of an arbitrarily chosen sensor s' and a prior distribution of the target velocity (see [33] for details).

The performance of the various methods is evaluated in terms of the Euclidean distance based OSPA metric [40] with a cutoff parameter of 200. For $S=3$ sensors and a detection probability (at the sensors) of $P_{\mathrm{d}}=0.8$, Fig. 2 shows the mean OSPA (MOSPA) error of the various methods versus time n. The error peaks at times $n=5$, 10, 15, 20, and 25 because of target births. It can be seen that very soon after a target birth, the proposed method as well as the IC-CPHD, MS-PHD, and MS-CPHD filters are able to reliably estimate the number of targets. Furthermore, the proposed method outperforms all the other methods. Its performance advantage over the IC-CPHD, MS-PHD, and MS-CPHD filters is mainly due to the potentially unreliable clustering scheme used in particle implementations of (C)PHD filters. This clustering scheme is especially prone to error if targets are in close vicinity, which explains the higher MOSPA error of the IC-CPHD, MS-PHD, and MS-CPHD filters around $n=100$, i.e., during the period where the target trajectories intersect in the ROI center. The IC-MB and IC-PHD filters are unable to reliably estimate the number of targets, which results in a significantly increased MOSPA error.

Fig. 3 shows the time-averaged MOSPA error (averaged over time steps $n\in\{50,\ldots,150\}$) versus P_{d} for $S=3$ sensors. As expected, the MOSPA error of all methods decreases with growing P_{d}. Fig. 4 shows the time-averaged MOSPA error versus the number of sensors S for $P_{\mathrm{d}}=0.6$. The MOSPA error of the MS-PHD and MS-CPHD filters increases for S larger than 5 because the chosen maximum numbers of subsets and partitions [17]—120 and 720, respectively—is too small for that case. (We note that larger maximum numbers of subsets and partitions would have resulted in excessive simulation runtimes.) Both Fig. 3 and Fig. 4 confirm the performance advantage of the proposed method over the considered reference methods. The poor performance of the IC-MB filter is related to the fact that the approximation used by the IC-MB filter is accurate only for high P_{d} [14], which can also be seen in Fig. 3.

V. Conclusion

We have proposed a belief propagation method for tracking an unknown number of targets using multiple sensors. The use of "augmented target states" including binary target indicators, an appropriate statistical model, and a redundant formulation

of data association uncertainty [28] resulted in low complexity and excellent scaling properties with respect to all relevant systems parameters. Our numerical results demonstrated that the proposed method can outperform previously proposed methods, including methods with a less favorable scaling behavior. In particular, we observed performance gains over various multisensor extensions of the PHD, CPHD, and multi-Bernoulli filters.

Possible directions for future research include extensions of the proposed method that adapt to time-varying environmental conditions and distributed variants for use in wireless sensor networks with communication constraints [41]. A particle-based implementation and further results will be presented in an extended journal version of this paper [33].

ACKNOWLEDGMENTS

F. Meyer and P. Braca are supported by the NATO Supreme Allied Command Transformation under project SAC000608 – Data Knowledge Operational Effectiveness. P. Willett is supported by the ONR under contract N000014-13-1-0231. F. Hlawatsch is supported by the FWF (grant P27370-N30) and by the European Commission under the National Sustainability Program (grant LO1401).

REFERENCES

[1] Y. Bar-Shalom and X.-R. Li, *Multitarget-Multisensor Tracking: Principles and Techniques*. Storrs, CT, USA: Yaakov Bar-Shalom, 1995.

[2] R. Mahler, *Statistical Multisource-Multitarget Information Fusion*. Norwood, MA, USA: Artech House, 2007.

[3] D. B. Reid, "An algorithm for tracking multiple targets," *IEEE Trans. Autom. Control*, vol. 24, no. 6, pp. 843–854, Dec. 1979.

[4] J. Vermaak, S. J. Godsill, and P. Perez, "Monte Carlo filtering for multi target tracking and data association," *IEEE Trans. Aerosp. Electron. Syst.*, vol. 41, no. 1, pp. 309–332, Jan. 2005.

[5] S. Deb, M. Yeddanapudi, K. Pattipati, and Y. Bar-Shalom, "A generalized S-D assignment algorithm for multisensor-multitarget state estimation," *IEEE Trans. Aerosp. Electron. Syst.*, vol. 33, no. 2, pp. 523–538, Apr. 1997.

[6] L. Y. Pao and C. W. Frei, "A comparison of parallel and sequential implementations of a multisensor multitarget tracking algorithm," in *Proc. ACC-95*, vol. 3, Seattle, WA, USA, Jun. 1995, pp. 1683–1687.

[7] D. Musicki and R. Evans, "Joint integrated probabilistic data association: JIPDA," *IEEE Trans. Aerosp. Electron. Syst.*, vol. 40, no. 3, pp. 1093–1099, Jul. 2004.

[8] D. Musicki and R. J. Evans, "Multiscan multitarget tracking in clutter with integrated track splitting filter," *IEEE Trans. Aerosp. Electron. Syst.*, vol. 45, no. 4, pp. 1432–1447, Oct. 2009.

[9] P. Horridge and S. Maskell, "Searching for, initiating and tracking multiple targets using existence probabilities," in *Proc. FUSION-09*, Seattle, WA, USA, Jul. 2009, pp. 611–617.

[10] R. Mahler, "Multitarget Bayes filtering via first-order multitarget moments," *IEEE Trans. Aerosp. Electron. Syst.*, vol. 39, no. 4, pp. 1152–1178, Oct. 2003.

[11] B.-N. Vo, S. Singh, and A. Doucet, "Sequential Monte Carlo methods for multitarget filtering with random finite sets," *IEEE Trans. Aerosp. Electron. Syst.*, vol. 41, no. 4, pp. 1224–1245, Oct. 2005.

[12] R. Mahler, "PHD filters of higher order in target number," *IEEE Trans. Aerosp. Electron. Syst.*, vol. 43, no. 4, pp. 1523–1543, Oct. 2007.

[13] B.-T. Vo, B.-N. Vo, and A. Cantoni, "Analytic implementations of the cardinalized probability hypothesis density filter," *IEEE Trans. Signal Process.*, vol. 55, no. 7, pp. 3553–3567, Jul. 2007.

[14] ——, "The cardinality balanced multi-target multi-Bernoulli filter and its implementations," *IEEE Trans. Signal Process.*, vol. 57, no. 2, pp. 409–423, Feb. 2009.

[15] P. Braca, S. Marano, V. Matta, and P. Willett, "Asymptotic efficiency of the PHD in multitarget/multisensor estimation," *IEEE J. Sel. Topics Signal Process.*, vol. 7, no. 3, pp. 553–564, Jun. 2013.

[16] R. Mahler, "The multisensor PHD filter: I. General solution via multitarget calculus," in *Proc. SPIE-09*, Orlando, FL, USA, Apr. 2009.

[17] S. Nannuru, M. Coates, M. Rabbat, and S. Blouin, "General solution and approximate implementation of the multisensor multitarget CPHD filter," in *Proc. IEEE ICASSP-15*, Brisbane, Australia, Apr. 2015, pp. 4055–4059.

[18] E. Delande, E. Duflos, P. Vanheeghe, and D. Heurguier, "Multi-sensor PHD: Construction and implementation by space partitioning," in *Proc. IEEE ICASSP-11*, Prague, Czech Republic, May 2011, pp. 3632–3635.

[19] S. Nagappa and D. Clark, "On the ordering of the sensors in the iterated-corrector probability hypothesis density (PHD) filter," in *Proc. SPIE-11*, Orlando, FL, USA, Apr. 2011, pp. 26–28.

[20] R. Mahler, "Approximate multisensor CPHD and PHD filters," in *Proc. FUSION-10*, Edinburgh, UK, Jul. 2010, pp. 26–29.

[21] S. Reuter, B.-T. Vo, B.-N. Vo, and K. Dietmayer, "The labeled multi-Bernoulli filter," *IEEE Trans. Signal Process.*, vol. 62, no. 12, pp. 3246–3260, Jun. 2014.

[22] B.-N. Vo, B.-T. Vo, and D. Phung, "Labeled random finite sets and the Bayes multi-target tracking filter," *IEEE Trans. Signal Process.*, vol. 62, no. 24, pp. 6554–6567, Dec. 2014.

[23] J. L. Williams, "Marginal multi-Bernoulli filters: RFS derivation of MHT, JIPDA and association-based MeMBer," *IEEE Trans. Aerosp. Electron. Syst.*, vol. 51, no. 3, pp. 1664–1687, Jul. 2015.

[24] F. R. Kschischang, B. J. Frey, and H.-A. Loeliger, "Factor graphs and the sum-product algorithm," *IEEE Trans. Inf. Theory*, vol. 47, no. 2, pp. 498–519, Feb. 2001.

[25] H. Wymeersch, *Iterative Receiver Design*. New York, NY, USA: Cambridge University Press, 2007.

[26] M. J. Wainwright and M. I. Jordan, "Graphical models, exponential families, and variational inference," *Found. Trends Mach. Learn.*, vol. 1, Jan. 2008.

[27] M. Chertkov, L. Kroc, F. Krzakala, M. Vergassola, and L. Zdeborová, "Inference in particle tracking experiments by passing messages between images," *Proc. Nat. Acad. Sci.*, vol. 107, no. 17, pp. 7663–7668, Apr. 2010.

[28] J. L. Williams and R. Lau, "Approximate evaluation of marginal association probabilities with belief propagation," *IEEE Trans. Aerosp. Electron. Syst.*, vol. 50, no. 4, pp. 2942–2959, Oct. 2014.

[29] P. Horridge and S. Maskell, "Real-time tracking of hundreds of targets with efficient exact JPDAF implementation," in *Proc. FUSION-06*, Florence, Italy, Jul. 2006, pp. 1–8.

[30] L. Chen, M. J. Wainwright, M. Cetin, and A. S. Willsky, "Data association based on optimization in graphical models with application to sensor networks," *Math. Comp. Model.*, vol. 43, no. 9–10, pp. 1114–1135, 2006.

[31] Z. Chen, L. Chen, M. Cetin, and A. S. Willsky, "An efficient message passing algorithm for multi-target tracking." in *Proc. FUSION-09*, Seattle, WA, USA, Jul. 2009, pp. 826–833.

[32] F. Meyer, P. Braca, P. Willett, and F. Hlawatsch, "Scalable multitarget tracking using multiple sensors: A belief propagation approach," in *Proc. FUSION-15*, Washington D.C., USA, Jul. 2015, pp. 1778–1785.

[33] ——, "A scalable algorithm for tracking an unknown number of targets using multiple sensors," 2016, in preparation.

[34] H. V. Poor, *An Introduction to Signal Detection and Estimation*. New York, NY: Springer, 1994.

[35] H. Wymeersch, J. Lien, and M. Z. Win, "Cooperative localization in wireless networks," *Proc. IEEE*, vol. 97, no. 2, pp. 427–450, Feb. 2009.

[36] P. O. Vontobel, "The Bethe permanent of a nonnegative matrix," *IEEE Trans. Inf. Theory*, vol. 59, no. 3, pp. 1866–1901, Mar. 2013.

[37] J. H. Kotecha and P. M. Djuric, "Gaussian particle filtering," *IEEE Trans. Signal Process.*, vol. 51, no. 10, pp. 2592–2601, Oct. 2003.

[38] R. Mahler, "The multisensor PHD filter: II. Erroneous solution via Poisson magic," in *Proc. SPIE-09*, Orlando, FL, USA, Apr. 2009.

[39] G. Gan, C. Ma, and J. Wu, *Data Clustering: Theory, Algorithms, and Applications*. Philadelphia, PA, USA: SIAM, 2007.

[40] D. Schuhmacher, B.-T. Vo, and B.-N. Vo, "A consistent metric for performance evaluation of multi-object filters," *IEEE Trans. Signal Process.*, vol. 56, no. 8, pp. 3447–3457, Aug. 2008.

[41] O. Hlinka, F. Hlawatsch, and P. M. Djuric, "Distributed particle filtering in agent networks: A survey, classification, and comparison," *IEEE Signal Process. Mag.*, vol. 30, no. 1, pp. 61–81, Jan. 2013.